Geophysical Journal International

Geophys. J. Int. (2013) doi: 10.1093/gji/ggt372

Geophysical Journal International Advance Access published October 11, 2013

Cretaceous to present kinematics of the Indian, African and Seychelles plates

Graeme Eagles* and Ha H. Hoang

Department of Earth Sciences, Royal Holloway University of London, Egham, Surrey, TW20 0EX, United Kingdom. E-mail: Graeme.Eagles@awi.de

Accepted 2013 September 16. Received 2013 September 13; in original form 2012 November 12

SUMMARY

An iterative inverse model of seafloor spreading data from the Mascarene and Madagascar basins and the flanks of the Carlsberg Ridge describes a continuous history of Indian–African Plate divergence since 84 Ma. Visual-fit modelling of conjugate magnetic anomaly data from near the Seychelles platform and Laxmi Ridge documents rapid rotation of a Seychelles Plate about a nearby Euler pole in Palaeocene times. As the Euler pole migrated during this rotation, the Amirante Trench on the western side of the plate accommodated first convergence and later divergence with the African Plate. The unusual present-day morphology of the Amirante Trench and neighbouring Amirante Banks can be related to crustal thickening by thrusting and folding during the convergent phase and the subsequent development of a spreading centre with a median valley during the divergent phase. The model fits FZ trends in the north Arabian and east Somali basins, suggesting that they formed in India–Africa Plate divergence. Seafloor fabric in and between the basins shows that they initially hosted a segmented spreading ridge that accommodated slow plate divergence until 71–69 Ma, and that upon arrival of the Deccan–Réunion plume and an increase to faster plate divergence rates in the period 69–65 Ma, segments of the ridge lengthened and propagated. Ridge propagation into the Indian continental margin led first to the formation of the Laxmi Basin, which accompanied extensive volcanism onshore at the Deccan Traps and offshore at the Saurashtra High and Somnath Ridge. A second propagation episode initiated the ancestral Carlsberg Ridge at which Seychelles–India and India–Africa Plate motions were accommodated. With the completion of this propagation, the plate boundaries in the Mascarene Basin were abandoned. Seafloor spreading between this time and the present has been accommodated solely at the Carlsberg Ridge.

Key words: Plate motions; Continental margins: divergent; Large igneous provinces; Kinematics of crustal and mantle deformation; Africa; Asia; Indian Ocean.

INTRODUCTION

The northwest (NW) Indian Ocean (Fig. 1) is a focus for oil and gas exploration, for studies of palaeogeography and palaeobiogeography (e.g. Lawver *et al*. 1998; Masters *et al*. 2006; Farke & Sertich 2013), for determining the timing and accommodation of continental collision between India and Eurasia (e.g. Aitchison *et al*. 2007), and for investigating the nature of interactions between mantle plumes and the lithosphere (e.g. van Hinsbergen *et al*. 2011; Eagles & Wibisono 2013). An integrated view of the regional plate tectonic development can help improve understanding in all of these fields, but currently must be built piecemeal from a range of plate- and basin-scale models, which can be mutually contradictory. Here we detail work that treats plate kinematic data from these settings in a shared context. Using a combination of iterative least squares and visual fitting procedures, we generate a plate rotation model that explains the present-day distribution of these data and minimizes complexity in terms of the number of plates it requires to exist simultaneously. We discuss it in terms of the development of plate boundaries accompanying the arrival of the Deccan–Réunion plume.

TECTONIC SETTING OF THE NW INDIAN OCEAN

The NW Indian Ocean grew in the regional context of divergence of the Indian and African plates. This has been appreciated since the identification of conjugate magnetic anomaly isochrons arrayed about the Carlsberg Ridge (McKenzie & Sclater 1971; Schlich & Fondeur 1974; Schlich *et al.* 1974; Norton & Sclater 1979; Schlich 1982; Molnar *et al*. 1988; Patriat & Segoufin 1988). Later, detailed mapping of these isochrons revealed that the seafloor produced

*Now at: Alfred Wegener Institute, Helmholtz Centre for Polar & Marine Research, Am Alten Hafen 26, Bremerhaven, D-27568, Germany.

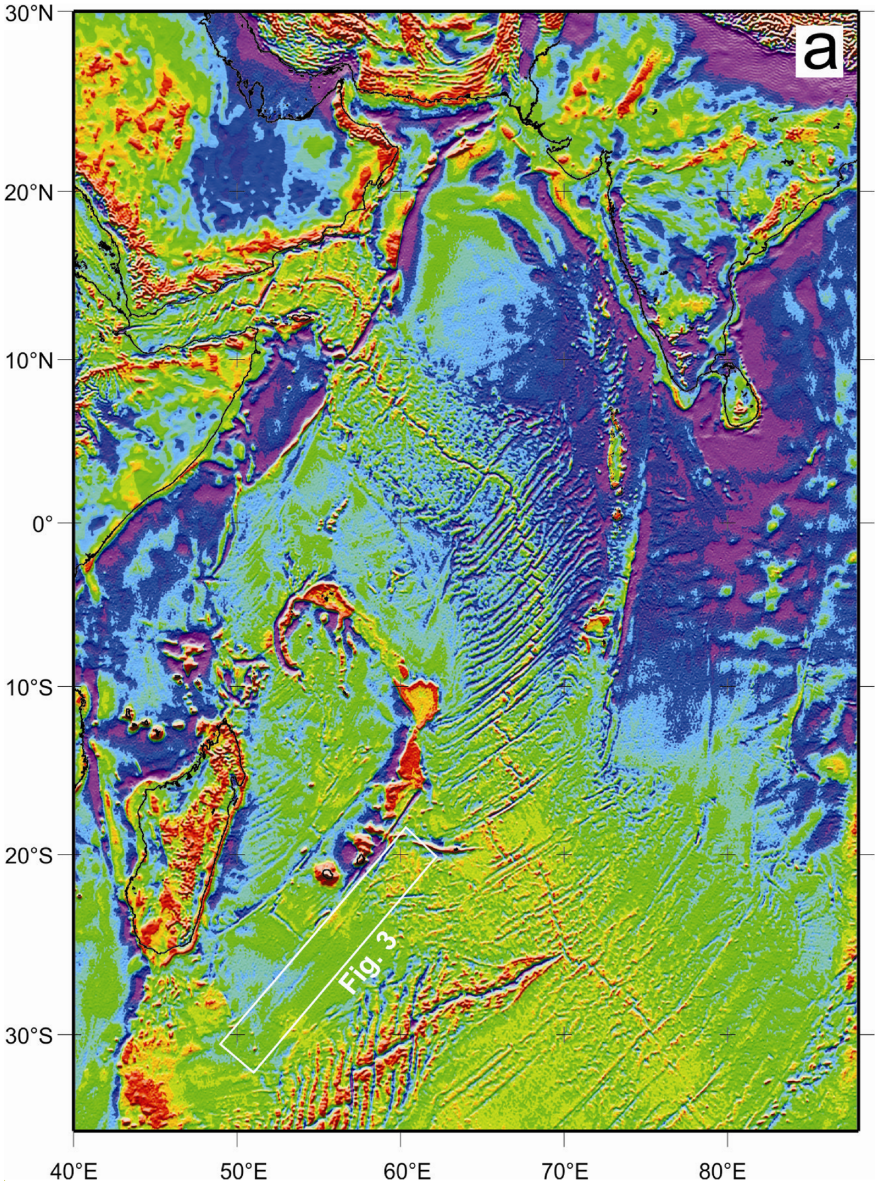

Figure 1. Satellite-derived free air gravity anomalies of the NW Indian Ocean (Sandwell & Smith 2009). Dark blue lines: fracture zones picked for modelling; light blue lines: active and extinct spreading centres; pink lines: features of the extended margins of Indian and African plates (gravity anomalies at continental shelf edges and trough on eastern edge of the West Somali Basin); dashed pink lines: seaward edges of gravity lows flanking the continental slopes. Pink area: Deccan Traps. Yellow: diffuse boundary zones of the Capricorn Plate at present-day. Other symbols: magnetic anomaly picks (see also key and Table 1). ATB, Amirante trench and banks; MP, Mascarene Plateau; N, Nazareth Bank; SM, Salha da Maya Bank; SP, Seychelles Plateau.

by the plate divergence is complicated somewhat by two large-scale processes. First, propagation and retreat of segments of the Carlsberg Ridge saw asymmetric accretion of material to the Indian and African plates, which has been related to the presence of Deccan plume mantle northeast of the ridge crest (Chaubey *et al*. 1998, 2002a; Dyment 1998). Second, it became apparent that much of the seafloor lying south of Sri Lanka had moved with respect to continental India as part of the so-called Capricorn component plate since Miocene or earlier times (Fig. 1; Wiens *et al*. 1985; Royer *et al*. 1997).

The Mascarene Basin hosts a record of plate motions that preceded spreading on the Carlsberg Ridge, which commenced at ~63 Ma (Collier *et al*. 2008). The Madagascan continental shelf edge on its western margin is marked by a linear, NNE-trending high-amplitude positive gravity anomaly that is more than 1000 km long (Fig. 1). Seawards of and parallel to this anomaly, a lower-amplitude negative anomaly suggests the presence of deep sedimentary basins at a continent–ocean transition that formed during continental extension. Further seawards still, magnetic isochrons in the south of the basin are identified in the range 34y–26 (~84–60 Ma) and arranged each side of a fossil median valley (Dyment 1991; Bernard & Munschy 2000). Plate kinematic reconstructions reveal how the basin opened about Euler poles situated to the NW (Müller *et al*. 2008; Eagles & Wibisono 2013; Gaina *et al*. 2013). As late Cretaceous stage poles for India–Africa divergence lay in this region too, and there is no evidence of other contemporary plate boundaries in the region, the southern Mascarene Basin is widely assumed to be a product of the early stages of India–Africa Plate divergence (Norton & Sclater 1979; Molnar *et al*. 1988; Bernard & Munschy 2000).

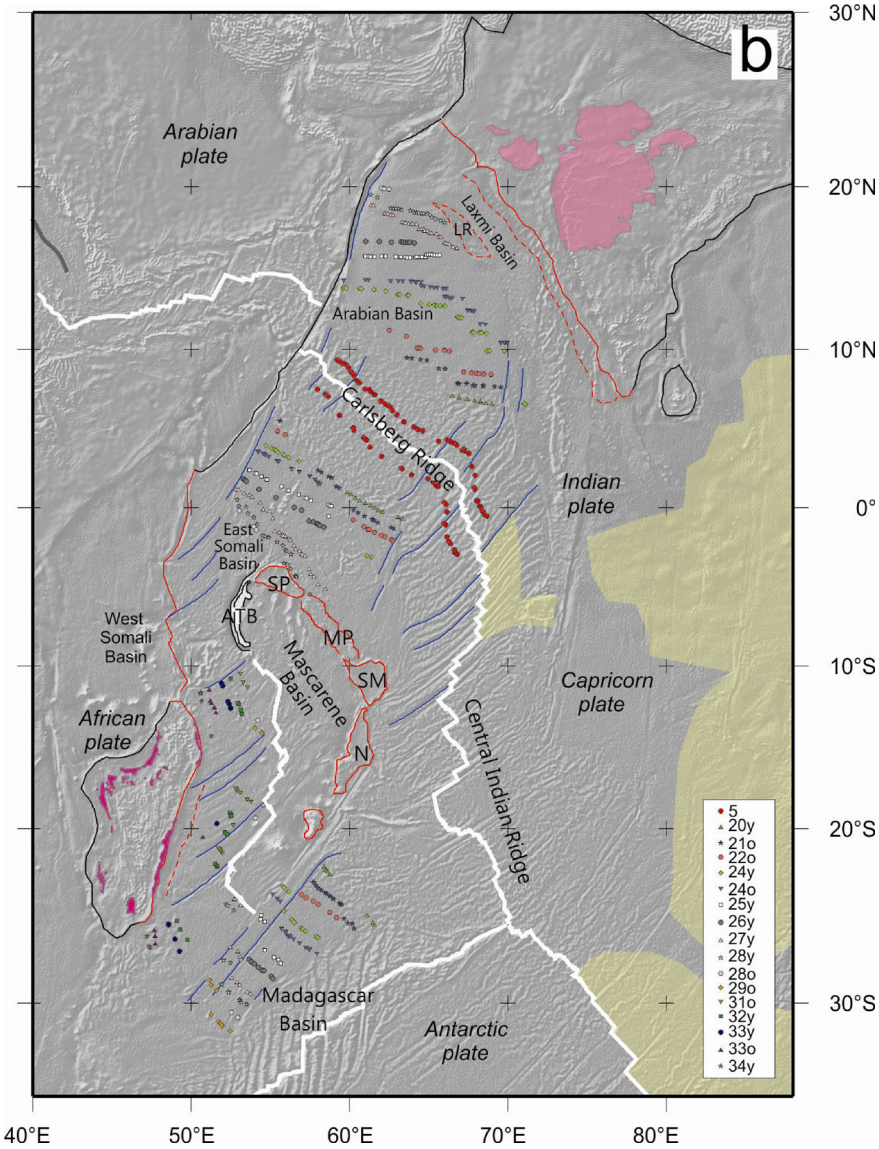

Figure 1 (*Continued*.)

On the eastern side of the Mascarene Basin, Proterozoic granitic basement is exposed on the Seychelles islands (Miller & Mudie 1961; Torsvik *et al*. 2001). Palaeomagnetic poles from Palaeogene igneous rocks from the Seychelles suggest that they experienced rotation as part of an independent plate (Ganerød *et al*. 2011). Consistent with this, the northern Mascarene Basin differs from the parts further south in that a prominent NNW-striking bathymetric trough known as the Amirante Trench occupies its median line. The trough and neighbouring Amirante Banks to the east are often presented as a subduction-related arc—trench system (Miles 1982; Masson 1984).

It has been suggested that the Seychelles platform forms the northern end of a continental conjugate to the eastern Madagascar margin that continues southwards beneath the Mascarene Plateau (Fig. 1; Francis & Shor 1966; Shields 1977; Plummer 1996; Torsvik *et al*. 2013). Isolation of the Mascarene Plateau in the Indian Ocean seems to have been achieved by ridge jumping or propagation events accompanying end-Cretaceous arrival of the Deccan–Réunion plume and the Indian Plate's subsequent northwards passage over it (Müller *et al*. 2001; Torsvik *et al*. 2013). The action of the plume saw the plateau come to be covered by a layer of Cenozoic basalt and related volcanic rocks, at least 830 m thick on Saya de Malha Bank and 160 m thick on Nazareth Bank, leading to an interpretation of the plateau as an oceanic large igneous province (Duncan & Hargraves 1990). This implies the conjugate to the eastern Madagascar margin lies at or off the western continental shelf of India, where the crust is well known to have experienced thinning (e.g. Yatheesh *et al*. 2006; Torsvik *et al*. 2013). Much of this shelf is characterised by a high-low gravity couplet like the one east of Madagascar (Fig. 1). The activity of the Deccan–Réunion hotspot as it passed southwards along the margin in Palaeocene times (O'Neill *et al*. 2003) has left features that lead to considerable uncertainty in the margin's crustal structure. Some studies attribute the margin an extraordinarily wide (>400 km) magma-rich transition zone, featuring embedded basins and bounding swells (Miles *et al*. 1998; Chaubey *et al*. 2002b; Krishna *et al*. 2006; Ajay *et al*. 2010). Others show a transition zone of more typical (<200 km) width that is bordered by narrow abandoned oceanic basins such as the Laxmi Basin and Gop Rift (Bhattacharya *et al*. 1994; Collier *et al*. 2008). The Laxmi Ridge on the seaward edge of the Laxmi Basin has been

interpreted as an abandoned microcontinent, whereas the Gop Rift appears only to have one continental margin, which also hosts a large igneous province (e.g. Naini & Talwani 1982; Singh 1999; Müller *et al*. 2001; Collier *et al*. 2008, 2009; Calvès *et al*. 2011).

PLATE KINEMATIC MODELLING APPROACH

Most pre-spreading reconstructions of the region are concerned to reunite the shapes of the conjugate Indian and Madagascan margins (e.g. Lawver *et al*. 1998; Gaina *et al*. 2007; Eagles & König 2008; Gibbons *et al*. 2013). This is attractive because it is intuitive, but on the other hand of limited use for reconstructing the growth of the ocean that followed on from the margins' separation. Molnar *et al*. (1988) and Cande *et al*. (2010) present alternative reconstructions that instead emphasise the intraoceanic markers that record the growth of the ocean at times beginning shortly after continental breakup between Madagascar and India, and the Seychelles and India. Both studies use the inversion procedure of Hellinger (1981) for reconstruction of conjugate plate boundary figures, and both had to overcome a number of obstacles specific to doing so in the NW Indian Ocean. The first is the relocation of most of the plate boundary from the Mascarene Basin to the Carlsberg Ridge. Another is the lack of consensus on late Cretaceous isochrons flanking the northern reaches of the Carlsberg Ridge. A third is that only one of the numerous fracture zones (FZs) in the NW Indian Ocean is located near dense-enough magnetic isochron data to be able to interpret the fossil transform faults that Hellinger's (1981) modelling technique uses as complementary constraints to the isochrons. Both Molnar *et al.* (1988) and Cande *et al.* (2010) alleviated these problems by enlarging the model to include data from the SW Indian and SE Indian ridges, and simultaneously solving for motions in a three-plate (India–Africa–Antarctica) circuit. The ultraslow spreading rate at the SW Indian Ridge however makes its magnetic isochrons difficult to identify and locate as confidently as elsewhere. A fourth problem is that independent Neogene motion of the Capricorn Plate (Fig. 1) will have displaced many data that first formed on the Indian Plate away from their original positions. To account for this, Cande *et al.* (2010) rotated affected data towards their original positions using the 20 Ma rotation of DeMets *et al.* (2005). DeMets *et al.* (2005) showed this rotation to be tightly constrained, but could not rule out earlier Capricorn–Indian motion. Because of this, it is possible that the back-rotated Capricorn Plate data are still located far enough away from their true original Indian Plate locations to introduce appreciable errors to Cande *et al.*'s (2010) model circuit.

Unlike Hellinger's (1981) method, our technique sets out to model entire FZs rather than only those parts that offset magnetic anomaly isochrons (Eagles 2004; Livermore *et al*. 2005). This introduces previously unusable local constraints on the model-spreading azimuth, and so allows us to avoid the use of isochron data from profiles recorded over slow or ultraslow spreading crust elsewhere in a plate circuit model. In addition, our approach is not restricted to the use of data in sets of conjugate pairs, so that we can avoid entirely the use of data from the Capricorn Plate whilst retaining the constraints from several hundred kilometres' length of palaeoridge recorded on the African Plate. Our model thus enjoys the tight constraints of data from long palaeo-plate boundaries, but remains free of the influence of any Capricorn Plate motion. The main difficulty this technique faces is related to asymmetric crustal accretion processes, which the fitting of non-conjugate magnetic anomalies in single spreading corridors cannot portray. Care must therefore be taken in assigning pairs of non-conjugate isochrons for the test rotations.

Interpretation of a data set for modelling

Consensus has existed on the presence of 65–42 Ma magnetic isochrons on the flanks of the Carlsberg Ridge since the recognition of the effects of ridge propagation processes by Dyment (1998) and Chaubey *et al.* (1998). We adhere to this consensus, digitising conjugate isochrons from Chaubey *et al.*'s (2002a) magnetic anomaly wiggle maps, updated very slightly with reference to Cande *et al.*'s (2010) more recent dataset (Fig. 1; Table 1). We added data for anomaly five from the maps of Royer *et al.* (1997), avoiding those from the Capricorn Plate and their African conjugates. FZs formed by the action of the Carlsberg Ridge are interpreted from satellite-derived free-air gravity anomalies (Sandwell & Smith 2009) by searching for lineaments with similar overall strikes to synthetic

Table 1. Labels for model rotations and magnetic anomalies, and their dates.

Model rotation label	Magnetic anomaly timescale label[a] and pick	Timescale age (Ma)[a]
5	5n.2n (peak)	10.51
20y	C20n (young edge)	41.59
21o	C21n (old edge)	47.24
22o	C22n (old edge)	49.43
24y	C24n.1n (young edge)	52.65
24o	C24n.3n (old edge)	53.81
25y	C25n (young edge)	56.67
26y	C26n (young edge)	58.38
27y	C27n (young edge)	61.65
28y	C28n (young edge)	63.10
28o	C28n (old edge)	64.13
29o	C29n (old edge)	65.12
30o	C30n (old edge)	67.70
31o	C31n (old edge)	68.73
32y	C32n.1n (young edge)	70.96
33y	C33n (young edge)	73.58
33o	C33n (old edge)	79.54
34y	C34n (young edge)	84.00

[a]Gradstein *et al*. (2004).

flowlines about Royer *et al.*'s (2002) and Molnar *et al.*'s (1988) sets of rotations.

Conflicting identifications of pre-65 Ma magnetic isochrons have been made from short magnetic profiles in the Laxmi Basin, between the Indian continental shelf and the proposed Laxmi Ridge microcontinent. Bhattacharya *et al.* (1994) modelled a two-sided set of anomalies (34–28–34) in the Laxmi Basin, using ultraslow spreading rates. Such rates would require independent motion of a 'Laxmi' Plate, making the anomalies unsuitable for use in our two-plate inversion technique. Eagles & Wibisono (2013) used the fast divergence rate of the Indian and African plates along with regional considerations to model a two-sided sequence with parts of anomalies 29–28–29 in the same data. This might be seen as consistent with the basin opening in India–Africa divergence, which was fast at that time. Potentially, therefore, data from the basin could contribute to our two-plate model. On balance, we consider the model sequence too short to be certain of either conclusion, and so do not include any data from the Laxmi Basin in our modelling.

A great diversity of tectonic interpretations has been proposed for the northern Arabian Basin lying immediately NW of the Laxmi Basin. NE-striking FZs have been interpreted in seismic data off the Pakistan–India continental margin (Malod *et al*. 1997; Calvès *et al*. 2011). Todal & Eldholm (1998) presented a continuation of the Carlsberg Ridge sequence to anomaly 31, which suggests the seafloor might have accreted between the Indian and African plates. Isochrons picked from these anomalies, together with the FZ locations, are potentially useful in a two-plate model for India—Africa divergence. In the east of the area, gravity and seismic data show an east-striking basement ridge called the Palitana Ridge between 63.5°E, 19.4°N and 65.6°E, 19.5°N (Malod *et al*. 1997), which has been interpreted from the axis or margin of a narrow abandoned basin referred to as the Gop basin or rift. Collier *et al.* (2008) and Yatheesh *et al.* (2009) compared magnetic anomaly profiles crossing the proposed basin to a variety of models, suggesting that the basin may host any one of a number of symmetrical magnetic isochron sequences: 31–29–31, 29–28–29, 32–31–30, 31–25–31 or 29–25–29. With the plate divergence directions and rates they require, all of these sets of identifications can imply the action of a third plate besides the African and Indian plates. As in the Laxmi Basin, therefore, we make no attempt to use any data from this part of the northern Arabian Basin.

Modelling of one long magnetic anomaly profile from the Madagascar Basin confirms the plausibility of the magnetic anomaly identifications presented and modelled on the African flank of the Central Indian Ridge by Cande *et al.* (2010), from whose maps we digitised the majority of magnetic isochron picks in the basin (Fig. 1). We added to these data a handful of picks for anomaly 28o on trackline data retrieved from the online archive of the U.S. National Geophysical Data Centre. In this basin, FZs are easy to trace from their appearance as linear troughs in free-air gravity anomalies, until they either terminate at or become confused with anomalies related to the Madagascar Ridge.

We used the data set of FZ and isochron picks on the African Plate from Eagles & Wibisono's (2013) model of seafloor spreading in the Mascarene Basin. The magnetic isochron data set is closely comparable to that of Bernard & Munschy (2000) except for a slightly different interpretation of ridge jumps close to the time of the Mascarene ridge's extinction. This interpretation enables the ridge's extinction to be viewed as having occurred geologically instantaneously all along the ridge. This view is preferable because diachronous extinction would need to have been accommodated by deformation of the Indian side of the Mascarene Basin, for which we see no unequivocal evidence. No Indian-side isochrons were used as these have been displaced from their original positions on the Indian Plate by their incorporation into the African Plate since Palaeogene times. This reduced the quantity of possible test rotations for chrons 30y and 30o to unusable numbers, meaning we were unable to calculate solutions for those times.

Finally, we picked a set of FZs in the east Somali basin that lie marginwards of anomaly 27, on the basis that their strikes and curvatures appear to continue the pattern of late Cretaceous African Plate FZs in the Mascarene Basin. These FZs are not associated with any reliable magnetic isochron picks, so it is difficult to tell whether or not they record relative motion of the Indian and African plates. We decided to test the possibility that these FZs do record India–Africa relative motion by incorporating them into the inverse modelling procedure.

Inverse model of India–Africa Plate divergence

The two-plate reconstruction technique in this study involves simultaneous fitting of FZs to synthetic ridge crest-offset flowlines, and of pairs of both conjugate and non-conjugate magnetic anomalies within spreading corridors (Eagles 2004; Livermore *et al*. 2005). A set of estimated reconstruction rotations is derived by iteratively reducing the misfits of magnetic anomalies rotated to conjugate and non-conjugate great circle targets, and of FZ picks to synthetic ridge-crest flowlines. Data uncertainties are treated as dominated by process-related noise and so as essentially unknown, rather than as in other schemes after *a priori* consideration of the reliability of navigation aids (Kirkwood *et al*. 1999). An overall uncertainty per data type is defined on the basis of the standard deviations of misfit values in the least squares solution.

Initially, we used only the FZs and conjugate magnetic anomaly data from the flanks of the Carlsberg Ridge to find a coarse solution that we could be sure to be unaffected by asymmetric accretion processes. Following this, we introduced the data from the Madagascar and Mascarene basins. In order to ensure that stage rotation angles calculated from these data are not misled by choices of rotations through distances shortened or lengthened during asymmetric crustal accretion by ridge jumping or propagation, we compared the widths of our anomaly isochrons to those in the unused conjugate sequences (Cande *et al*. 2010; Eagles & Wibisono 2013). Such a check is not possible for anomaly 34y, which is only present on the African side of the Mascarene Basin. Consequently, we cannot be certain that the chron 34y rotation angle is not under- or overestimated. By this point, the fits of isochrons 27y and 28y near the Seychelles Platform to their conjugates south of the Laxmi Ridge stood out as markedly less precise than those in the rest of the model. Given the locations of these data, this imprecision is consistent with independent evidence for rotation of a separate Seychelles Plate (Ganerød *et al*. 2011), and so we excluded the data from further use in the model. Finally, we introduced the picks of old FZs from the east Somali basin. Introducing these FZs to the model as a final step allowed us to test the hypothesis that they recorded relative motions of the same India–Africa plate pair as in the rest of the model. We consider the hypothesis to have passed this test because the introduction did not cause large changes to the model solution, and did not reduce its overall misfit or visual quality for times prior to chron 27y.

The mean errors and standard deviations of misfit populations in the solution are (neglecting outliers under the assumption the misfit populations ought to adopt Gaussian distributions) 0.1 and

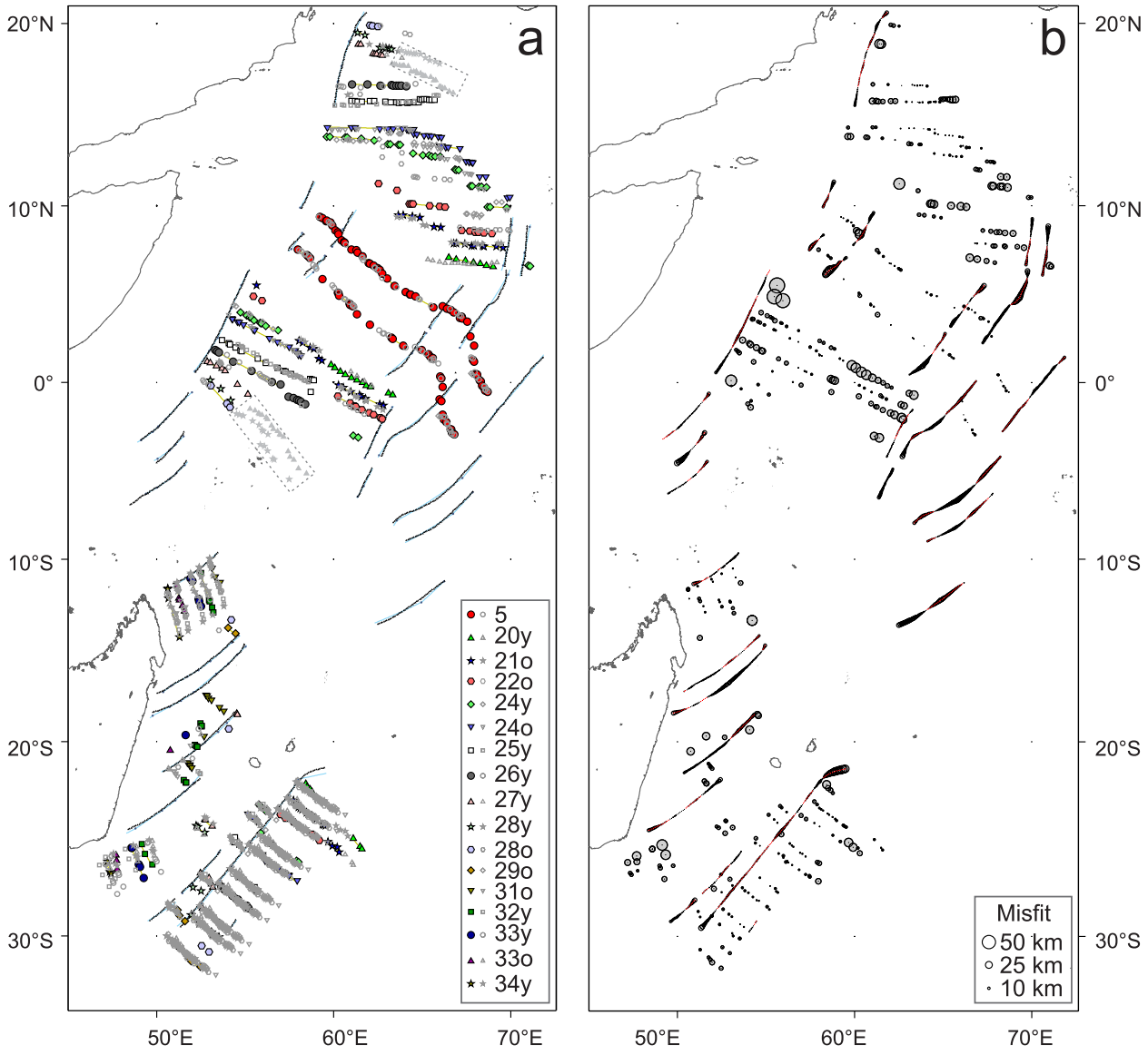

Figure 2. (a) Fits of model elements to FZ and magnetic data. Small black triangles: FZ data picks. Coloured symbols: magnetic anomaly picks. Smaller grey outline symbols: rotated magnetic anomaly picks. Small grey-filled symbols in boxes: 27y and 28y picks excluded from inversion as records of Seychelles—Africa motion. Blue lines: segments of synthetic flowlines, (b) misfits in the model. The size of each circle is proportional to the misfit between the data point at its centre and the corresponding model element. Misfits for magnetic data that undergo multiple rotations to multiple targets are rms values. For clarity, misfit circles for the magnetic isochron picks are filled.

7.8 km to magnetic data and 0.5 and 6.3 km to FZ data or (without the Gaussian assumption) 0.5 and 13.8 km to magnetic data and 0.3 and 7.2 km to FZ data. Values like these are typical for this technique, and consistent with estimates of the likely errors in pick locations with either navigational or process-related causes. Fig. 2 shows that these errors are geographically evenly distributed within the data set, and that the solution produces an acceptable likeness to the data set. The calculation of synthetic flowline targets means that none of the FZs are assigned explicitly to conjugates; the solution nonetheless reveals the same pairs of FZs to be conjugates that were assigned as such by Cande *et al.* (2010). Fig. 3 shows in more detail that our rotations produce synthetic flowlines through Cretaceous to mid-Eocene seafloor that are smoother and more reminiscent of the FZs than those produced by earlier rotation sets, and so may be viewed as internally more consistent. The poor fit between the sharp bend at chron 20y in our synthetic flowline and the FZ is a consequence of the long modelled stage between chrons 20y and 5, and is not representative of all the modelled FZs. If suitable data were available, a better fit for the full set of FZ bends might be achieved by modelling rotations for chrons between 20y and 5.

Fig. 4 and Table 2 show that the solution's India–Africa rotations and their 95 per cent confidence ellipses are about poles located in the same region as those of previous studies. The oldest rotations are about a tight cluster of poles. They produce a model of the Mascarene Basin that is qualitatively very similar to that of Eagles & Wibisono (2013), and so are consistent with the assumption that the basin opening records Africa—India Plate motion. In our model, these older rotations are part of a continuous sequence for Africa—India motions, and so not subject to the errors that might arise from addition of rotations based on Carlsberg Ridge data to those based on Mascarene Basin data. Within this cluster of older rotation poles, those for rotations 33y, 32y and 31o show a reversed geographical

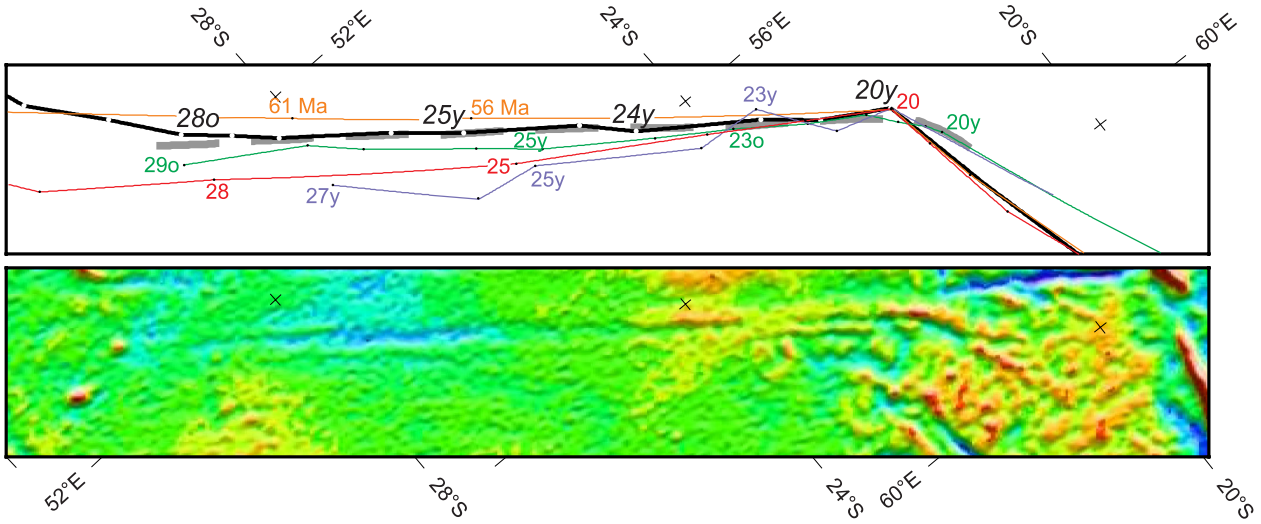

Figure 3. Comparison of flowlines in various plate kinematic models of the NW Indian Ocean to a long FZ picked from satellite-derived free-air gravity anomalies (bottom; location in Fig. 1). The fracture zone trace is shown with a thick dashed grey line in the top panel, to which the model flowlines compared to it are about rotations derived in this study (black), Molnar *et al.* (1988; red), Royer *et al.* (2002; blue), Torsvik *et al.* (2013; amber) and Cande *et al.* (2010; green). Labels are for numerical ages in Ma, or isochrons as listed in those publications.

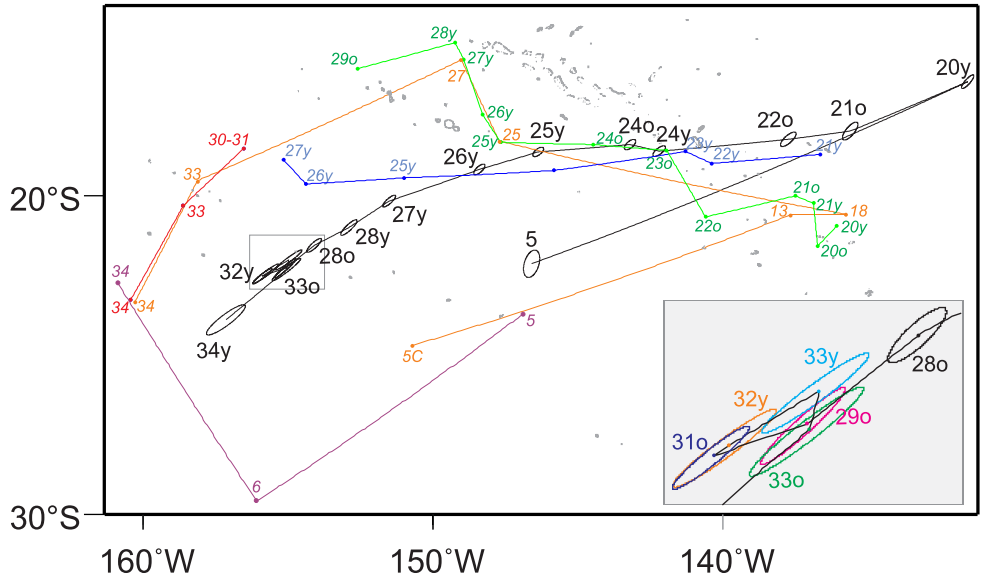

Figure 4. Locations of the solution rotation poles and their 95 per cent confidence ellipses. Other rotation poles for India–Africa motion are shown in green: Cande *et al.* (2010); blue: Royer *et al.* (2002); red: Molnar *et al.* (1988); mauve: Torsvik *et al.* (2008) and amber: (Torsvik *et al*. 2013). All labels are magnetic anomaly timescale numbers. Inset: detail of the clustered portion of the finite rotation pole progression path.

progression in comparison to most of the rest of the series. There is no comparable reversal in Eagles & Wibisono's (2013) sequence of poles for opening of the Mascarene Basin. That model differs from ours by omitting FZ data from the East Somali basin, but including conjugate magnetic anomaly and FZ data in the eastern, Indian, side of the Mascarene Basin. More critically, the distribution of magnetic isochron picks in the basin means that Eagles & Wibisono (2013) were able to constrain rotations for chrons 30o and 30y, giving their model of Mascarene Basin growth a greater temporal resolution than is possible with our model geometry. We suspect therefore that the reversal in the sequence of finite rotations in our model is less likely to reflect an important change in the location of stage poles than it is to be an artefact related to smoothing of its post-31o stage by the inability to calculate rotations for chrons 30o and 30y.

Rotation of the Seychelles Plate and the origin of the Amirante trench and banks

Palaeogene and older palaeomagnetic poles from the Seychelles islands have been interpreted in terms of a period of anticlockwise rotation by a small plate bearing the islands (Torsvik *et al*. 2001; Ganerød *et al*. 2011). The Amirante Trench and neighbouring Amirante Banks are likely to have formed part of an African-Plate boundary with this Seychelles Plate, because they skirt the Seychelles platform and form a link between Palaeogene magnetic isochrons on the African flank of the Carlsberg Ridge and in the northern Mascarene Basin. This boundary has been interpreted as an inactive subduction zone in view of the Amirante trench and banks' superficial resemblance to a subduction-related arc-trench system (Miles 1982; Masson 1984). However, there is no strong

Table 2. Finite rotation parameters (India with respect to Africa) and 95 per cent confidence regions for the full model (Fig. 5).

Model rotation parameters			95 per cent confidence ellipsoid, 1σ great circle degrees				
Longitude	Latitude	Angle	Axis 1	Axis 2	Axis 3	Azimuth	Label
−146.59	−22.19	4.71	0.18	0.10	0.03	72.46	C5
−131.53	−16.20	25.24	0.15	0.04	0.03	48.19	C20y
−135.58	−17.84	25.77	0.18	0.06	0.03	49.15	C21o
−137.70	−18.11	27.21	0.16	0.05	0.03	41.71	C22o
−142.14	−18.48	29.95	0.13	0.04	0.03	37.83	C24y
−143.16	−18.28	31.72	0.11	0.04	0.02	39.33	C24o
−146.34	−18.53	34.43	0.11	0.04	0.02	37.11	C25y
−148.38	−19.12	35.90	0.11	0.04	0.03	41.62	C26y
−151.51	−20.15	38.05	0.12	0.03	0.03	42.13	C27y
−152.90	−21.01	38.81	0.16	0.04	0.03	43.26	C28y
−154.18	−21.67	39.80	0.15	0.05	0.04	43.00	C28o
−155.23	−22.37	41.38	0.20	0.03	0.03	42.09	C29o
−155.96	−22.61	45.16	0.21	0.11	0.02	40.32	C31o
−155.78	−22.49	47.52	0.29	0.10	0.03	36.46	C32y
−154.99	−22.05	50.05	0.31	0.11	0.03	35.82	C33y
−155.03	−22.33	52.64	0.33	0.11	0.03	36.97	C33o
−155.04	−22.43	53.63	0.41	0.11	0.07	37.12	C34y

subduction signature in the N-MORB chemistry of rocks dredged from the Amirante Banks (Tararin & Lelikov 2000; Stephens *et al*. 2009) and neither the detailed nor long-wavelength morphology of the Amirante Trench resemble a typical subduction trench formed by flexural loading of the lithosphere at a convergent plate boundary (Miles 1982; Damuth & Johnson 1989).

Above, we noted that we excluded picks of isochrons 28y and 27y near the Seychelles platform and Laxmi Ridge from our model of India–Africa motions because of their large misfits. In detail, the Indian-side isochrons' strikes are rotated clockwise away from their targets near the Seychelles. The timing and sense of these misalignments are consistent with the anticlockwise palaeomagnetic rotation of Ganerød *et al.* (2011). The isochrons thus are likely to describe the shape of a Seychelles–India ridge and so can be used to quantify the motion of the Seychelles Plate. To do this, within the context of our India–Africa plate model, we search for rotations of the Seychelles-side isochrons that produce good visual fits to their Indian-side conjugates at the same time as agreeing with the palaeomagnetic constraints from the Seychelles (Fig. 5; Table 3). Notably, clockwise finite rotations that reconstruct continuous pre-28y plate convergence at the Amirante Trench, which must take place about a rotation pole south of the trench, tend to further separate the Seychelles–India ridge isochrons (Figs 5c and d). We conclude that the idea of continuous pre-28y subduction at the Amirante Trench is not helpful for determining the rotation of the Seychelles Plate.

The isochrons' misalignment is effectively rectified by applying clockwise rotations to the Seychelles Plate data around Euler poles a shorter distance to their southwest (Figs 5a and b). The rotation for 27y is well constrained by the alignment of numerous data in two segments on both plates. In contrast the 28y rotation, sought whilst attempting to minimize changes to the rotation parameters for chron 27y, is constrained by fewer than ten data in one segment owing to the absence of magnetic anomaly data in which to follow chron 28y southeast of the Laxmi Ridge. Both rotations use large angles that lie within the range of Ganerød *et al.*'s (2011) chron 28o palaeomagnetic rotation (29.4° ± 12.9°). The 28y–27y stage rotation calculated between the two occurs about a pole at 6.7°S, 51.3°E; it lies almost within the plate boundary whose action it describes. Relationships like this are suggested to be typical

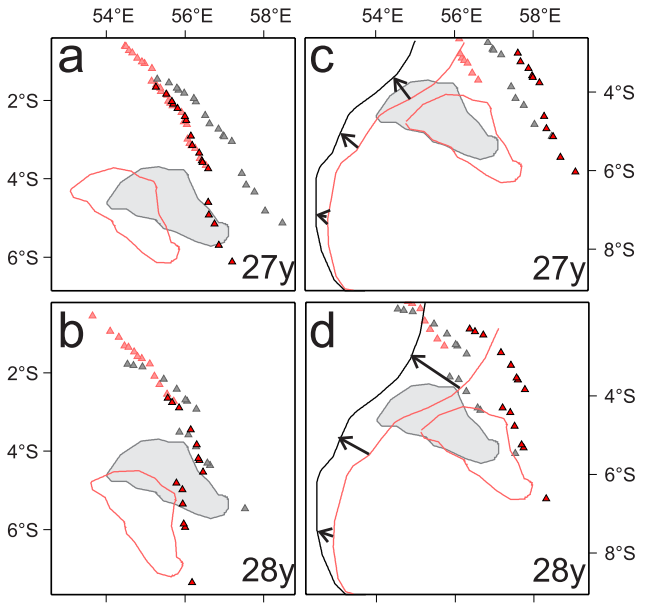

Figure 5. Visual fit modelling for relative locations of Seychelles and African plates at chrons 27y and 28y. Grey-filled outline and triangles: present-day positions of Seychelles platform and neighbouring picks of the magnetic anomaly being reconstructed. Rose-coloured triangles: positions of the Indian Plate conjugates to these picks after rotation about the relevant pole from Table 2. Red-filled triangles and outline: the Seychelles–side picks and Seychelles platform after rotations listed in Table 3. In (a) and (b) anomalies 27y and 28y are reconstructed for satisfactory visual fits. In (c) and (d), the anomalies are rotated about poles that also produce continuous plate convergence (heavy arrows) or subduction at the Amirante Trench (black and red lines: before and after rotation).

of so-called diffuse plate boundaries, where they are necessary to meet the requirements for relative motion to be slow and for plate boundary torques to be balanced (Zatman *et al*. 2001). Plummer (1996) proposed similar boundary-contained poles in his concept of Cretaceous Amirante Trench tectonics. The rotation pole for chron 27y lies at the furthest northern point of the boundary, consistent with Zatman *et al.*'s (2001) finding that rotation poles move along

Table 3. Finite rotation parameters (Seychelles with respect to Africa).

Rotation	Longitude	Latitude	Angle	Label
Fig. 5(a)	−125.39	1.46	17.48	27y
Fig. 5(b)	−126.49	4.02	31.49	28y
Fig. 5(c)	−126.5	9.0	10.0	27y
Fig. 5(d)	−126.5	9.0	15.0	28y

diffuse boundaries in response to changes in the torque balance caused by the boundary's localisation. Based on the assumption that the Amirante Trench acted as part of a diffuse plate boundary, then, the earliest Palaeogene stage poles for Africa–Seychelles motion may have been situated closer to its southern end.

Fig. 6 summarizes the implications these rotations have for motion between the Africa and Seychelles plates, which we assume for simplicity to have been expressed solely along the Amirante Trench and a line stretching northeast of it towards a triple junction on the Carlsberg Ridge. The 28y–27y stage rotation produces a maximum of 65 km of extensional motion on the southern Amirante Trench, increasing to 75 km of convergence its northern end, via an intervening strike-slip segment. Off the Seychelles platform, the same rotation implies 150 km of convergence. These numbers, calculated from two finite rotations that use angles within the uncertainty range of Ganerød *et al.*'s (2011) palaeomagnetic rotation, but using independent constraints, serve as a minimum estimate of Seychelles–Africa convergence. For a maximum estimate, we assume that additional pre-28y Seychelles–Africa rotation occurred about a stage pole at the southern end of the trench, by an amount sufficient to produce a total Seychelles Plate rotation at the top end of Ganerød *et al.*'s (2011) uncertainty estimate. This yields convergence by ∼15 km at the southern end of the Amirante Trench, increasing to 60 km at the northern end, and 120 km at the Seychelles platform.

The minimum total convergence estimate is thus 0–150 km (increasing between the central Amirante Trench and NW Seychelles platform) and the maximum is 15–270 km (increasing from the southern end of the Amirante Trench to the NW Seychelles platform). The minimum estimated convergence completes in 1.45 Myr, whereas the maximum estimate requires 2.5 Myr. Away from the continental Seychelles platform, convergence would have affected young (<5 Myr old) oceanic lithosphere of both the African and Seychelles plates. Whilst modelling studies show that >100 km of convergence may be enough to force the initiation of subduction in some settings, the buoyancy and weakness of young oceanic lithosphere ensures the shortest time required to do so is 5 Myr (e.g. Leng & Gurnis 2011). Because of this, we consider the likelihood of subduction initiation having been forced on the Amirante Trench to be small. Folding and thrusting accompanying the plate convergence, rather than volcanism related to subduction, may therefore better explain the crustal thickening modelled in gravity data over the Amirante Banks (Miles 1982). North of the Seychelles platform, the corrugated nature of the seafloor may in part also be attributable to deformation of the young oceanic plate during the same period of convergence.

After the convergent phase, our chron 27y rotation implies a period of divergence (Fig. 6). From this, the Amirante Trench in its present form is interpretable as the median valley of a mid-ocean ridge that accommodated plate divergence varying in the range 100–240 km from north to south. If the angular rate of this rotation was the same as that during the preceding stage, then the Seychelles Plate would have ceased independent rotation at 59.9 Ma. This time falls within the youngest magnetic chron recorded in the southern Mascarene Basin, the reversed polarity part (61.65–58.74 Ma) of chron 26 (Bernard & Munschy 2000; Eagles & Wibisono 2013), suggesting simultaneous abandonment of the Seychelles Plate and the ridge in the Mascarene Basin. As the assumption of a constant angular rate is unlikely to be strong, bearing in mind the large changes in the boundary's nature, a more conservative estimate of the time range in which the Seychelles Plate was incorporated into the African Plate may thus be 59.9–58.74 Ma. With this estimate, integrated half spreading rates on this late-stage Seychelles—Africa ridge may have been slow to fast from north to south along the ridge (26.5–68.6 km Myr^{-1}, with extinction at 59.9 Ma) or slow to intermediate from north to south (17.2–41.5 km Myr^{-1}, with extinction at 58.74 Ma).

Whatever its timing, the morphology of the Amirante Trench suggests its extinction occurred whilst it was accommodating plate divergence at slow or even ultraslow seafloor spreading rates. Fig. 7 compares the morphologies of the trench to the median valleys at parts of the active ultraslow SW Indian and extinct (since 25 Ma) slow Ægir ridges, which show features typical of their classes (Small 1998). All three are ∼30 km wide bathymetric troughs that gently curve over their >500 km lengths. All three show median valley topography, with steep parallel sidewalls forming bathymetric relief in excess of 1000 m. The basement surfaces, buried beneath ∼1 km thick sediment layers at the Amirante Trench and Ægir Ridge, are rugged but not tilted (Damuth & Johnson 1989; Uenzelmann-Neben *et al.* 1992; Dick *et al.* 2003). All three troughs have sections that

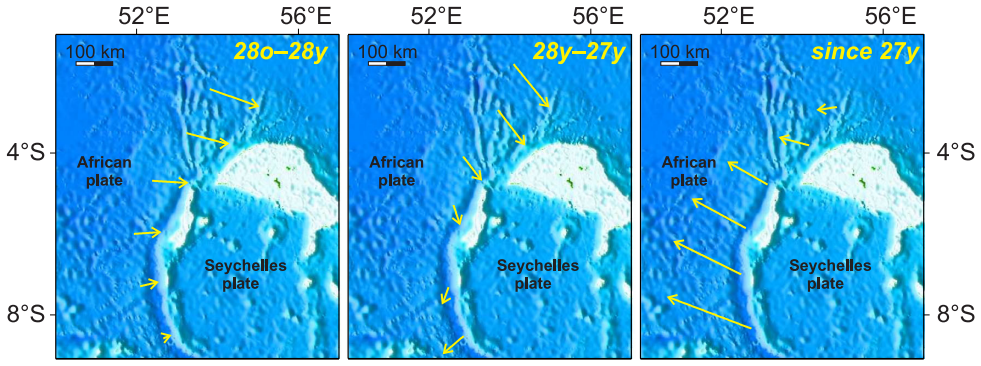

Figure 6. Relative Seychelles–Africa plate motions according to the estimated rotations of Table 3 and Fig. 5. The background image uses ETOPO-1 global topography (Amante & Eakins 2009) to highlight the location of the Palaeogene Amirante Trench plate boundary between the African and Seychelles plates. Yellow arrows show the motion of points on the African Plate now at the arrow heads during the stated time period. The 28o–28y motions are a maximum estimate based on the largest permissible palaeomagnetic rotation of Ganerød *et al.* (2011).

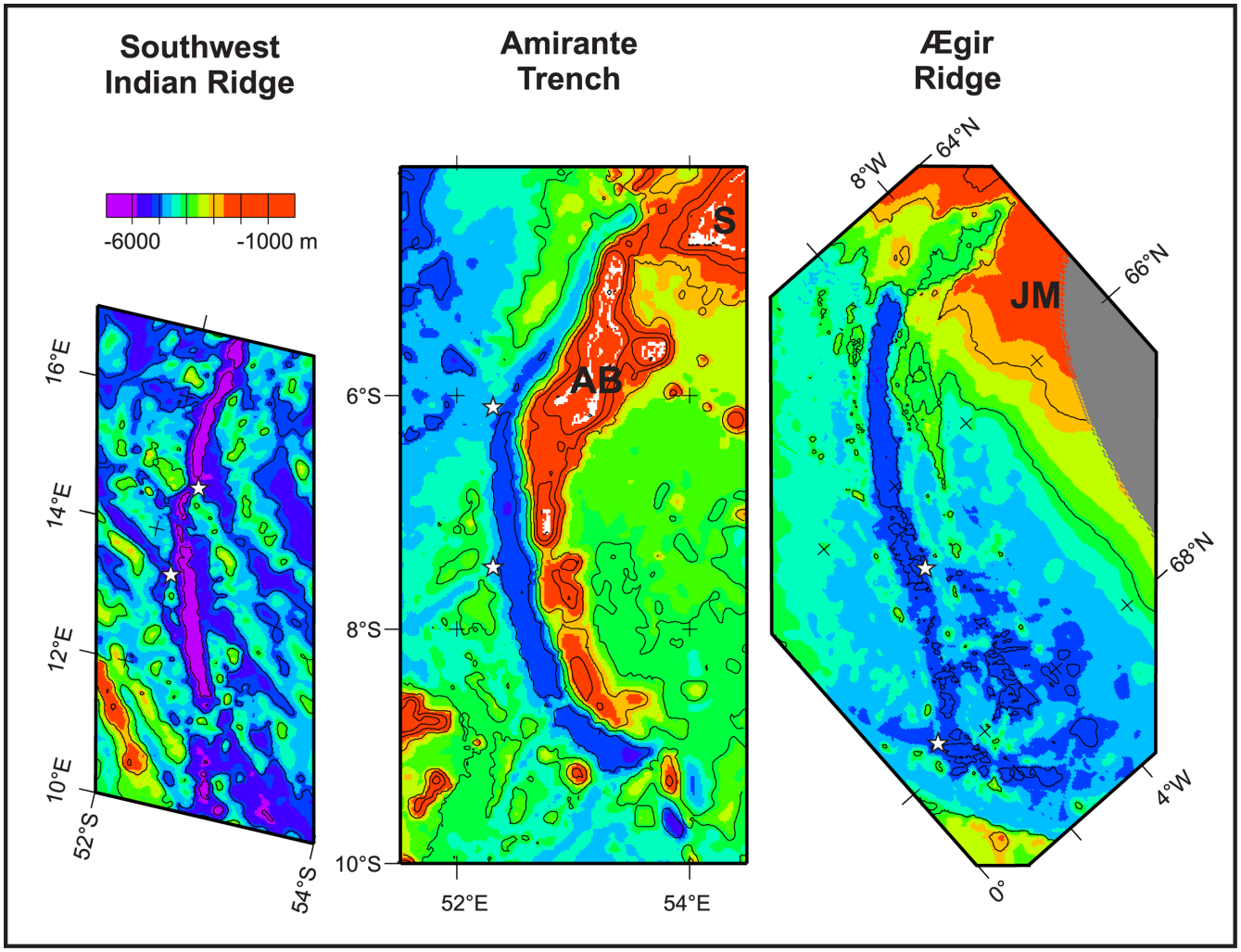

Figure 7. Bathymetric comparison of the Amirante Trench (centre) to the median valleys at the extinct slow-spreading Ægir (right) and active ultraslow spreading Southwest Indian (left) ridges. The Ægir and Southwest Indian ridge bathymetry have been adjusted for thermal subsidence according to the plate cooling model of Stein & Stein (1992) so that they appear as if they were embedded in seafloor of the same age as the Amirante Trench. AB, Amirante Banks; JM, Jan Mayen microcontinent; S, Seychelles Plateau. Stars: FZ intersections with oblique ridge-crest segments.

are oblique to the FZs on their flanks, a feature of ultraslow ridges (Dick *et al*. 2003). Based on an oceanic subsidence model (Stein & Stein 1992) and their current depths, the median valley floors at the Ægir and SW Indian ridges would lie 4.7 and 6.3 km deep 65 Myr after their extinctions. The Amirante Trench, deepening southwards along its length from 5.2 to 5.7 km, falls comfortably within this range. The similarities between the Amirante Trench and a slow spreading ridge suggest therefore that the end of independent motion of the Seychelles Plate may indeed have occurred somewhat later than 59.9 Ma (the time we extrapolated for above).

These considerations suggest plate boundary processes ceased in the Amirante Trench at 59.9–58.74 Ma. The main challenge to this suggestion is the ∼52 Ma (Eocene) age of a gabbro from a population of slightly enriched N-MORB rocks dredged from the trench's eastern wall (Tararin & Lelikov 2000; Stephens *et al*. 2009). If the date is reliable, perhaps the most simple explanation for the gabbro and its moderate enrichment is as a result of small-scale melting of fertile mantle inhomogeneities below the extinct ridge. Based on studies of various ridges, melt production in this way has been suggested to continue for up to 10 Myr after ridge extinction (Batiza 1977; Clague *et al*. 2009; Haase *et al*. 2011). Alternatively, the gabbro might be seen as a volumetrically small melt product of plume mantle that migrated along the base of the lithosphere to the thickness contrast at the Amirante trench and banks. The gabbro is not the only instance of Eocene intraplate melting in the region. DSDP hole 240 stopped in basalt dated to Eocene times using microfossils in chalk xenoliths (Simpson *et al*. 1974), post-dating the expected late Cretaceous basement and overlying its signal in seismic refraction modelling by some 500 m (Francis *et al*. 1966). Its eruption or emplacement onto or into Eocene sediments can be related to activity of the Comores plume, whose Eocene location was close by O'Neill *et al*. (2003). If the Amirante Banks gabbro is related to the same plume, then its source mantle would have migrated 500 km southwards, a distance well within the range suggested for plume mantle in other settings (e.g. Ebinger & Sleep 1998).

DISCUSSION: THE NORTH ARABIAN AND EAST SOMALI BASINS

Fig. 8 is a reconstruction of satellite-derived free-air gravity anomalies (Sandwell & Smith 2009) made using the chron 27y rotations from Tables 2 and 3, and Eagles & Wibisono (2013). It illustrates

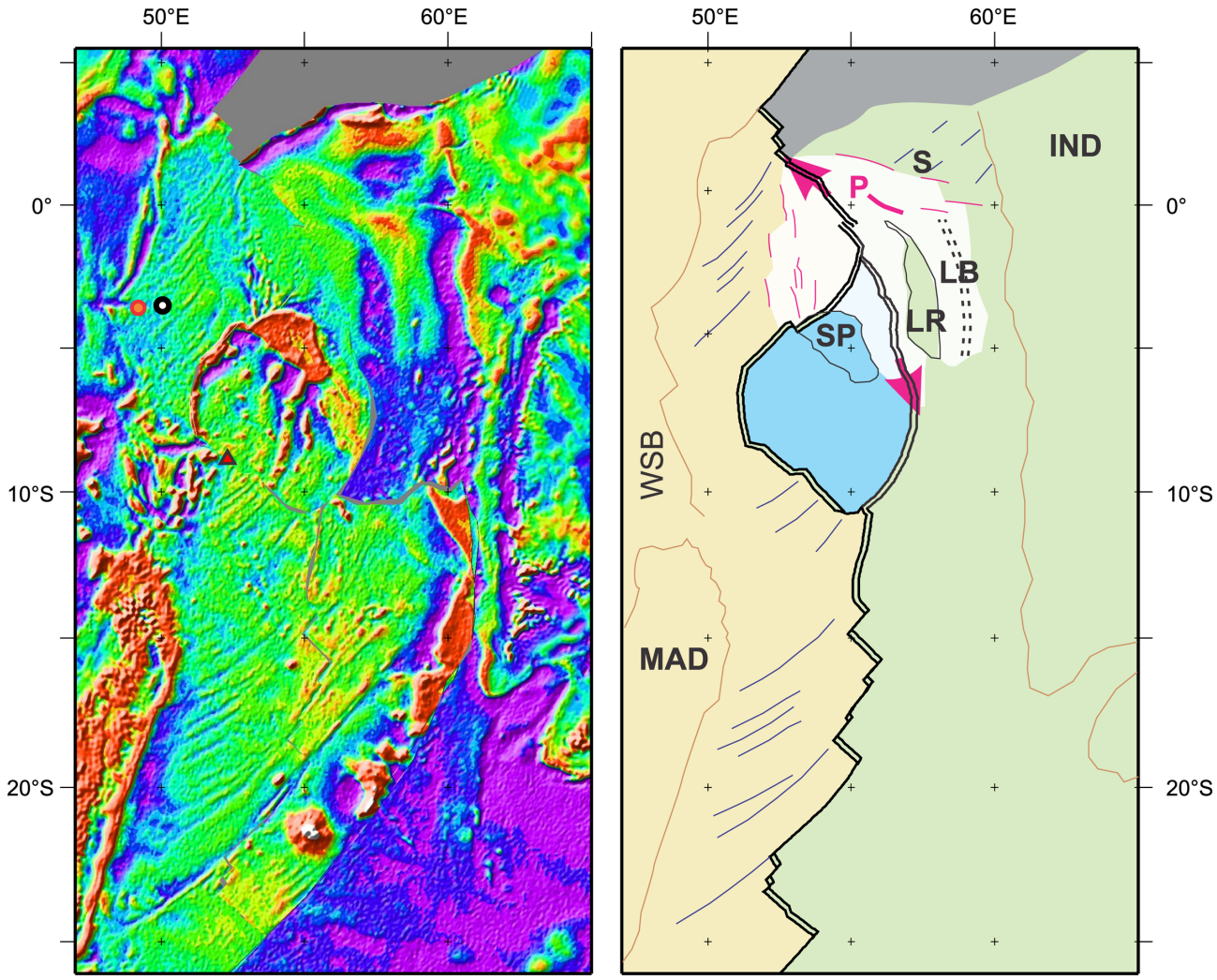

Figure 8. (a) Reconstruction of free-air gravity data to chron 27y, in present-day African reference frame. Red triangle: dredge site in Amirante Trench, red disk: 50 Ma model location of Comores plume (O'Neill *et al*. 2003), White disk: DSDP Site 240. (b) Interpretation of Fig. 8(a): IND, India; LB, Laxmi Basin; LR, Laxmi Ridge; MAD, Madagascar; P, Palitana Ridge; S, Somnath–Saurashtra volcanic province; SP, Seychelles platform; WSB, West Somali Basin. Mauve arrows: propagating ridge segment ends. Mauve lines: oblique lineaments in wedges of smooth seafloor; blue lines: FZs; brown lines: extended margins; grey fill: subducted or shortened seafloor; buff fill: African Plate at 27y; green fill: Indian Plate at 27y; blue fill: Seychelles Plate at 27y; lightened fill: areas of smooth gravity fabric.

a time, 61.65 Ma, soon after the main phase of Deccan Traps volcanism (Courtillot *et al*. 1986) and during the rapid rotation of the Seychelles Plate. We complete an interpretation of the Seychelles Plate's boundaries using a southward continuation of the Seychelles–India ridge that bends gradually into a SW orientation. The absence of a fossil median valley in the gravity data is consistent with spreading at fast plate divergence rates that can be calculated using the rotations in Tables 2 and 3.

The reconstruction shows closely spaced FZs in the east Somali basin. Earlier we saw that the shapes of these FZs and their apparent continuity of trend with FZs in the western Mascarene Basin are as would be expected to have formed in the African Plate by the action of transform faults on a late Cretaceous Indian–African ridge (Fig. 2). Linear features in the seismic basement and gravity field of the north Arabian basin hint at the presence of a set of NE-trending FZs there too. Signals from these features are shortened and obscured by the effects of the overlying Somnath Ridge–Saurashtra High volcanic complexes (Malod *et al*. 1997; Carmichael *et al*. 2009; Calvès *et al*. 2011). Despite this, the NE trend of the lineaments permits their interpretation as Indian-Plate conjugates to the east Somali basin FZs. Notwithstanding the absence of consensus on the identities of magnetic isochrons in the east Somali and north Arabian basins therefore, we conclude the most parsimonious view of the basins is as products of late Cretaceous divergence between the Indian and African plates.

Closely spaced transforms like these can develop in response to the weak melt supply below and characteristic deformation of the cold, brittle oceanic crust typical of mid-ocean ridges that operate between slowly (<28 mm yr^{-1}) diverging plates or over depleted mantle (e.g. Sempéré *et al*. 1991; Bell & Buck 1992; Small 1998). The region's various Cretaceous and Palaeogene large igneous provinces strongly suggest that its mantle was largely fertile, so that its closely-spaced FZs are most simply interpretable in terms of periods of slow plate divergence. Consistent with the locations of closely spaced FZs marginward of isochrons 28 and 27 in the east Somali and north Arabian basins, our rotations show that such a period ended some time between 71 and 69 Ma (Fig. 9). As the closely spaced FZs needed to form in cold crust, we

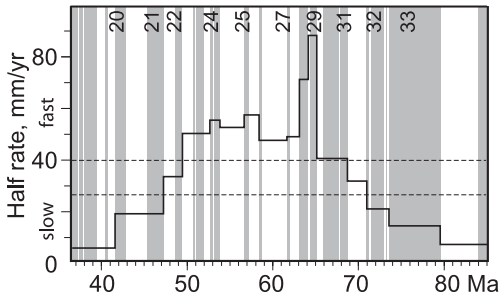

Figure 9. Half spreading rates on a length of India–Africa ridge (now part of the Carlsberg Ridge at 8.4N, 58.7E) that would have acted to form parts of the north Arabian and east Somali basins, calculated from the rotations in Table 2.

conclude that 71–69 Ma is also the range of maximum possible ages for the Somnath–Saurashtra volcanic rocks overlying them in the north Arabian basin. Interpreted close links between this volcanism and volcanic features of the northern Laxmi Basin (Corfield *et al*. 2010), together with recent modelling of that basin's magnetic anomalies (Eagles & Wibisono 2013), suggest the volcanism accompanied the main episode of Deccan Trap eruptions.

Fig. 9 shows fast spreading rates in the east Somali and north Arabian would first have been reached in the period 69–65 Ma (chrons 31–29). Simultaneously, the Deccan–Réunion plume arrived beneath the region, bringing with it the conditions for a supply of excess melt (Basu *et al*. 1993). Under these conditions, plate divergence is expected to be accommodated dominantly by igneous crust development, with the development of fewer large normal faults than at slower rates (Small 1998). The smooth gravity fabric flanking the reconstructed Carlsberg Ridge is a signal of these processes. Consistent with this, magnetic isochron 28o on both plates lies well within this area of smooth gravity, which continues into the Laxmi Basin where anomalies 29 and 28 are identifiable (Eagles & Wibisono 2013). The smooth gravity fabric forms a NW-pointing wedge centred on the NW Carlsberg Ridge, and a SE-pointing wedge defined by the edges of the Seychelles platform and Laxmi Ridge. We interpret these wedges as indications that the increase in plate divergence rate accompanied lengthening of the ridge by propagation.

A number of subtle gravity lineaments within the area of smooth fabric are arrayed oblique to the reconstructed ridge crest. We suggested earlier that some of these lineaments may be related to convergent deformation in Seychelles–Africa Plate convergence. Another lineament, on the Indian Plate, marks the Palitana Ridge, which Malod *et al.*'s (1997) seismic data and Yatheesh *et al.*'s (2009) magnetic anomaly grid show to be a steep-sided east-striking basement ridge, up to 1.5 km high. This relief is reminiscent of the oblique ridges flanking the Reykjanes Ridge south of Iceland, which have been interpreted in terms of episodes of ridge propagation in the presence of excess melt supply (Hey *et al*. 2010). Given these similarities, we suggest more of the oblique ridges of the east Somali and north Arabian basins may also be related to repeated ridge propagation episodes that occurred to accommodate the increasing spreading rates and excess melt production from the Deccan–Réunion plume mantle.

CONCLUSIONS

Our plate kinematic model describes the tectonic development of the NW Indian Ocean using a continuous set of rotation parameters for times since 84 Ma. It provides a context within which to enhance resolution in our knowledge of the motion of the Seychelles Plate using simple visual fit modelling of magnetic anomaly isochrons. We find that the small Seychelles Plate rotated rapidly anticlockwise with respect to the neighbouring African Plate about nearby Euler poles in the period 64–59 Ma. Early on, these Euler poles were situated within the plate's boundary to the African Plate so that the boundary's southern reaches experienced convergence. Comparison with geodynamic model experiments suggests that the time span and amount of this convergence would not have favoured forced subduction initiation. The Amirante Banks may therefore be related to crustal thickening by folding and faulting during the convergence. Later, the Seychelles–Africa Euler pole migrated northwards along the margin as the margin started to accommodate plate divergence. The end of this period of divergence, and thus its rate, is poorly constrained from the plate kinematic modelling. The morphology of the Amirante Trench, however, resembles that of a slow or ultraslow spreading centre and suggests that at least the final stages of divergence happened at slow or ultraslow rates.

Prior to these events, it is more difficult to draw confident conclusions about the origins of the northern Arabian and east Somali basins because of the complexity and paucity of their magnetic anomaly signals. FZ traces in both regions are however consistent with their accretion between the same two plates, India and Africa, as the Mascarene Basin further south. An area of smooth seafloor that formed after these FZs can be interpreted as a product of rapid ridge propagation that occurred to accommodate accelerated plate divergence and increasing melt supply in the pre-Deccan 69–65 Ma period. These propagations saw the Mascarene Basin progressively abandoned in favour of short-lived spreading in the Laxmi Basin, and the subsequent spreading at the Carlsberg Ridge.

ACKNOWLEDGEMENTS

We thank Royal Holloway University of London for funding. Jérôme Dyment and one anonymous reviewer made constructive comments for which we are similarly grateful.

REFERENCES

Aitchison, J.C., Ali, J.R. & Davis, A.M., 2007. When and where did India and Asia collide? *J. geophys. Res.,* **112,** B05423, doi:10.1029/2006JB00470.

Ajay, K.K., Chaubey, A.K., Krishna, K.S., Gopala Rao, D. & Sar, D., 2010. Seaward dipping reflectors along the SW continental margin of India: evidence for volcanic passive margin, *J. Earth Syst. Sci.,* **119,** 803–813.

Amante, C. & Eakins, B.W., 2009. *ETOPO1 1 Arc-Minute Global Relief Model: Procedures, Data Sources and Analysis,* NOAA Technical Memorandum NESDIS NGDC-24, 19 pp.

Basu, A.R., Renne, P.R., Dasgupta, D.K., Teichmann, F. & Poreda, R.J., 1993. Early and late alkali igneous pulses and a high-He-3 plume origin for the Deccan flood basalts, *Science,* **261,** 902–906.

Batiza, R., 1977. Petrology and chemistry of Guadalupe Island: an alkalic seamount on a fossil ridge crest, *Geology,* **5,** 760–764.

Bell, R.E. & Buck, W.R., 1992. Crustal control of ridge segmentation inferred from observations of the Reykjanes Ridge, *Nature,* **357,** 583–586.

Bernard, A. & Munschy, M., 2000. Were the Mascarene and Laxmi Basins (western Indian Ocean) formed at the same spreading centre? *Comptes Rendus de l'Academie des Sciences – Series IIA. Earth planet. Sci.,* **330,** 777–783.

Bhattacharya, G.C., Chaubey, A.K., Murty, G.P.S., Srinivas, K., Sarma, K., Subrahmanyam, V. & Krishna, K.S., 1994. Evidence for sea-floor spreading in the Laxmi Basin, northeastern Arabian Sea, *Earth planet. Sci. Lett.,* **125**(1–4), 211–220.

Calvès, G., Schwab, A.M., Huuse, M., Clift, P.D., Gaina, C., Jolley, D., Tabrez, A.R. & Inam, A., 2011. Seismic volcanostratigraphy of the western Indian rifted margin: The pre-Deccan igneous province, *J. geophys. Res.,* **116,** B01101, doi:10.1029/2010JB000862.

Cande, S.C., Patriat, P. & Dyment, J., 2010. Motion between the Indian, Antarctic and African plates in the early Cenozoic, *Geophys. J. Int.,* **183**. 127–149.

Carmichael, S.M. *et al.*, 2009. Geology and hydrocarbon potential of the offshore Indus Basin, Pakistan, *Petrol. Geosci.,* **15,** 107–116.

Chaubey, A.K., Bhattacharya, G.C., Murty, G.P.S., Srinivas, K., Ramprasad, T. & Gopala Rao, D., 1998. Early Tertiary seafloor spreading magnetic anomalies and paleo-propagators in the northern Arabian Sea, *Earth planet. Sci. Lett.,* **154,** 41–52.

Chaubey, A.K., Dyment, J., Bhattacharya, G.C., Royer, J.Y., Srinivas, K. & Yatheesh, V., 2002a. Paleogene magnetic isochrons and paleo-propagators in the Arabian and Eastern Somali basins, northwest Indian Ocean, in *The Tectonic and Climatic Evolution of the Arabian Sea Region,* Vol. **195,** pp. 71–85, eds Clift, P.D., Kroon, D., Gaedicke, C. & Craig, J., Geol. Soc. London Spec. Publ.

Chaubey, A.K., Gopala Rao, D., Srinivas, K., Ramprasad, T., Ramana, M.V. & Subrahmanyam, V., 2002b. Analyses of multichannel seismic reflection, gravity and magnetic data along a regional profile across the central-western continental margin of India, *Mar. Geol.,* **182,** 303–323.

Clague, D.A., Paduan, J.B., Duncan, R.A., Huard, J.J., Davis, A.S., Castillo, P.R., Lonsdale, P. & DeVogelaere, A., 2009. Five million years of compositionally diverse, episodic volcanism: construction of Davidson Seamount atop an abandoned spreading center, *Geochem. Geophys. Geosyst.,* **10,** Q12009, doi:10.1029/2009GC002665.

Collier, J.S., Sansom, V., Ishizuka, O., Taylor, R.N., Minshull, T.A. & Whitmarsh, R.B., 2008. Age of Seychelles–India break-up, *Earth planet. Sci. Lett.,* **272,** 264–277.

Collier, J.S., Minshull, T.A., Hammond, J.O.S., Whitmarsh, R.B., Kendall, J.-M., Sansom, V., Lane, C.I. & Rumpker, G., 2009. Factors influencing magmatism during continental breakup: new insights from a wide-angle seismic experiment across the conjugate Seychelles-Indian margins, *J. geophys. Res.,* **114,** B03101, doi:10.1029/2008JB005898.

Corfield, R.I., Carmichael, S., Bennett, J., Akhter, S., Fatimi, M. & Craig, T., 2010. Variability in the crustal structure of the West Indian Continental Margin in the Northern Arabian Sea, *Petrol. Geosci.,* **16,** 257–265.

Courtillot, V., Besse, J., Vandamme, D., Montigny, R., Jaeger, J.J. & Cappetta, H., 1986. Deccan flood basalts at the Cretaceous/Tertiary boundary? *Earth planet. Sci. Lett.,* **80,** 361–374.

Damuth, J.E. & Johnson, D.A., 1989. Morphology, sediments and structure of the Amirante Trench, Western Indian Ocean: implications for trench origin, *Mar. Petrol. Geol.,* **6,** 232–242.

DeMets, C., Gordon, R.G. & Royer, J.-Y., 2005. Motion between the Indian, Capricorn, and Somalian plates since 20 Ma: implications for the timing and magnitude of distributed deformation in the equatorial Indian ocean, *Geophys. J. Int.,* **161,** 445–468.

Dick, H.J.B., Lin, J. & Schouten, H., 2003. An ultraslow-spreading class of ocean ridge, *Nature,* **426,** 405–412.

Duncan, R.A. & Hargraves, R.B., 1990. $^{40}Ar/^{39}Ar$ geochronology of basement rocks from the Mascarene Plateau, the Chagos Bank, and the Maldives Ridge, in *Proceedings of the ODP, Sci. Results,* Vol. **115,** pp. 43–51, eds Duncan, R.A. *et al.*, Ocean Drilling Program.

Dyment, J., 1991. Structure et evolution de la lithosphere oceanique dans l'ocean Indien: apport des anomalies magnetiques, *PhD thesis*, Univ. Louis Pasteur, Strasbourg, France, 374 pp.

Dyment, J., 1998. Evolution of the Carlsberg Ridge between 60 and 45 Ma: Ridge propagation, spreading asymmetry, and the Deccan–Reunion hotspot, *J. geophys. Res.,* **103**(B10), 24 067–24 084.

Eagles, G., 2004. Tectonic evolution of the Antarctic–Phoenix plate system since 15 Ma, *Earth planet. Sci. Lett.,* **217,** 97–109.

Eagles, G. & König, M., 2008. A model of plate kinematics in Gondwana breakup, *Geophys. J. Int.,* **173,** 703–717.

Eagles, G. & Wibisono, A.D., 2013. Ridge push, mantle plumes, and the speed of the Indian plate, *Geophys. J. Int.,* **194,** 670–677.

Ebinger, C.J. & Sleep, N.H., 1998. Cenozoic magmatism throughout east Africa resulting from impact of a single plume, *Nature,* **395,** 788–791.

Farke, A.A. & Sertich, J.J.W., 2013. An Abelisauroid Theropod Dinosaur from the Turonian of Madagascar, *PLoS ONE,* **8,** e62047.

Francis, T.J.G. & Shor, G.G. Jr., 1966. Seismic refraction measurements in the northwest Indian Ocean, *J. geophys. Res.,* **71,** 427–449.

Francis, T.J.G., Davies, D. & Hill, M.N., 1966. Crustal structure between Kenya and the Seychelles, *Phil. Trans. Roy. Soc. Lond.,* **A259,** 227–239.

Gaina, C., Müller, R.D., Brown, B., Ishihara, T. & Ivanov, S., 2007. Breakup and early seafloor spreading between India and Antarctica, *Geophys. J. Int.,* **170,** 51–170.

Gaina, C., Torsvik, T.H., van Hinsbergen, D.J.J., Medvedev, S., Werner, S.C. & Labails, C., 2013. The African Plate: a history of oceanic crust accretion and subduction since the Jurassic, *Tectonophysics,* **604**, 4–25.

Ganerød, M. *et al.*, 2011. Palaeoposition of the Seychelles microcontinent in relation to the Deccan Traps and the Plume Generation Zone in Late Cretaceous–Early Palaeogene time, in *The Formation and Evolution of Africa: A Synopsis of 3.8 Ga of Earth History,* Vol. **357,** pp. 229–252, eds Van Hinsbergen, D.J.J., Buiter, S.J.H., Torsvik, T.H., Gaina, C. & Webb, S.J., Geological Society, London, Special Publications.

Gibbons, A.D., Whittaker, J.M. & Müller, R.D., 2013. The breakup of East Gondwana: assimilating constraints from Cretaceous ocean basins around India into a best-fit tectonic model, *J. geophys. Res.,* **118,** 808–822.

Gradstein, F.M. *et al.*, 2004. *A Geologic Time Scale 2004,* Cambridge Univ. Press, 589 pp.

Haase, K.M., Beier, C., Fretzdorff, S., Leat, P.T., Livermore, R.A., Barry, T.L., Pearce, J.A. & Hauff, F., 2011. Magmatic evolution of a dying spreading axis: evidence for the interaction of tectonics and mantle heterogeneity from the fossil Phoenix Ridge, Drake Passage, *Chem. Geol.,* **280,** 115–125.

Hellinger, S.J., 1981. The uncertainties of finite rotations in plate tectonics, *J. geophys. Res.,* **86,** 9312–9318.

Hey, R., Martinez, F., Höskuldsson, Á. & Benediktsdóttir, Á., 2010. Propagating rift model for the V-shaped ridges south of Iceland, *Geochem. Geophys. Geosyst.,* **11,** Q03011, doi:10.1029/2009GC002865.

Kirkwood, B.H., Royer, J.-Y., Chang, T. & Gordon, R., 1999. Statistical tools for estimating and combining finite rotations and their uncertainties, *Geophys. J. Int.,* **137,** 408–428.

Krishna, K.S., Gopala Rao, D. & Sar, D., 2006. Nature of the crust in the Laxmi Basin, western continental margin of India, *Tectonics,* **25,** TC1006, doi:10.1029/2004TC001747.

Lawver, L.A., Gahagan, L.M. & Dalziel, I.W.D., 1998. A tight fit early Mesozoic Gondwana: a plate reconstruction perspective, *Mem. Natl. Inst. Polar Res. Spec. Issue.,* **53,** 214–229.

Leng, W. & Gurnis, M., 2011. Dynamics of subduction initiation with different evolutionary pathways, *Geochem. Geophys. Geosyst.,* **12,** Q12018, doi:10.1029/2011GC003877.

Livermore, R.A., Nankivell, A.P., Eagles, G. & Morris, P., 2005. Paleogene opening of Drake Passage, *Earth planet. Sci. Lett.,* **236,** 459–470.

Malod, J.A., Droz, L., Mustafa Kamal, B. & Patriat, P., 1997. Early spreading and continental to oceanic basement transition beneath the Indus deep sea fan: Northeastern Arabian Sea, *Mar. Geol.,* **141,** 221–235.

Masson, D.G., 1984. Evolution of the Mascarene Basin, Western Indian Ocean, and significance of the Amirante Arc, *Mar. Geophys. Res.,* **6,** 365–382.

Masters, J.C., de Wit, M.J. & Asher, R.J., 2006. Reconciling the origins of Africa, India and Madagascar with vertebrate dispersal scenarios, *Folia Primatol.,* **77,** 399–418.

McKenzie, D. & Sclater, J.G., 1971. The evolution of the Indian Ocean since the late Cretaceous, *Geophys. J. R. astr. Soc.,* **25,** 437–528.

Miles, P.R., 1982. Gravity models of the Amirante Arc, western Indian Ocean, *Earth planet. Sci. Lett.,* **61,** 127–135.

Miles, P.R., Munschy, M. & Segoufin, J., 1998. Structure and early evolution of the Arabian Sea and East Somali Basin, *Geophys. J. Int.,* **134,** 876–888.

Miller, J.A. & Mudie, J.D., 1961. Potassium–argon age determinations on granite from the islands of Mahé in the Seychelles archipelago, *Nature,* **192,** 1174–1175.

Molnar, P., Pardo-Casas, F. & Stock, J., 1988. The Cenozoic and Late Cretaceous evolution of the Indian Ocean: uncertainties in the reconstructed positions of the Indian, African and Antarctic plates, *Basin Res.,* **1,** 23–40.

Müller, R.D., Gaina, C., Roest, W. & Hansen, D.L., 2001. A recipe for microcontinent formation, *Geology,* **29,** 203–206.

Müller, R.D., Sdrolias, M., Gaina, C. & Roest, W.R., 2008. Age, spreading rates, and spreading asymmetry of the world's ocean crust, *Geochem. Geophys. Geosyst.,* **9,** Q04006, doi:10.1029/2007GC001743.

Naini, B.R. & Talwani, M., 1982. Structural framework and the evolutionary history of the continental margin of Western India, in *Studies in Continental Margin Geology,* pp. 167–191, eds Waktins, J.S. & Drake, C.L., AAPG.

Norton, I.O. & Sclater, J.G., 1979. A model for the evolution of the Indian Ocean and the breakup of Gondwanaland, *J. geophys. Res.,* **84,** 6803–6830.

O'Neill, C., Müller, R.D. & Steinberger, B., 2003. Geodynamic implications of moving Indian Ocean hotspots, *Earth planet. Sci. Lett.,* **215,** 151–168.

Patriat, P. & Segoufin, J., 1988. Reconstruction of the Central Indian Ocean, *Tectonophysics,* **155,** 211–234.

Plummer, P.S., 1996. The Amirante ridge/trough complex: response to rotational transform rift/drift between Seychelles and Madagascar, *Terra Nova,* **8,** 34–47.

Royer, J.-Y., Gordon, R.G., DeMets, C. & Vogt, P.R., 1997. New limits on the motion between India and Australia since chron 5 (11 Ma) and implications for lithospheric deformation in the equatorial Indian Ocean, *Geophys. J. Int.,* **129,** 41–74.

Royer, J.Y., Chaubey, A.K., Dyment, J., Bhattacharya, G.C., Srinivas, K., Yatheesh, V. & Ramprasad, T., 2002. Paleogene plate tectonic evolution of the Arabian and Eastern Somali basins, in *The Tectonic and Climatic Evolution of the Arabian Sea Region,* pp. 7–23, eds Clift, P.D., Croon, D., Gaedicke, C. & Craig, J., Geological Society.

Sandwell, D.T. & Smith, W.H.F., 2009. Global marine gravity from retracked Geosat and ERS-1 altimetry: ridge segmentation versus spreading rate, *J. geophys. Res.,* **114,** B01411, doi:10.1029/2008JB006008.

Schlich, R., 1982. The Indian Ocean: aseismic ridges, spreading centers and basins, in *The Ocean Basins and Margins,* pp. 51–147, eds Nairn, A.E. & Stehli, F.G., Plenum.

Schlich, R. & Fondeur, C., 1974. Anomalies crétacées dans le bassin des Mascareignes, *C. R. Acad. Sci. Paris,* **D278,** 541–544.

Schlich, R. *et al.*, 1974. Site 239, in *Initial Reports of the Deep Sea Drilling Project,* Vol. **25,** pp. 25–64, eds Simpson, E.S.W. & Schlich, R., U.S. Government Printing Office.

Sempéré, J.-C., Palmer, J., Christie, D.M., Phipps Morgan, J. & Shor, A.N., 1991. Australian—Antarctic discordance, *Geology,* **19,** 429–432.

Shields, O., 1977. A Gondwanaland reconstruction for the Indian Ocean, *J. Geol.,* **85,** 236–242.

Simpson, E.S.W. *et al.*, 1974. Site 240, in *Initial Reports of the Deep Sea Drilling Project,* Vol. **25,** pp. 65–86, eds Simpson, E.S.W. & Schlich, R., U.S. Government Printing Office.

Singh, A.P., 1999. The deep crustal accretion beneath the Laxmi Ridge in the northeastern Arabian Sea: the plume model again, *J. Geodyn.,* **27,** 609–622.

Small, C., 1998. Global systematics of mid-ocean ridge morphology, in *Faulting and Magmatism at Mid-Ocean Ridges,* Vol. **106,** pp. 1–25, eds Buck, W.R., Delaney, P.T., Karson, J.A. & Lababrielle, Y., American Geophysical Union Monograph.

Stein, C. & Stein, S., 1992. A model for the global variation in oceanic depth and heat flow with lithospheric age, *Nature,* **359,** 123–128.

Stephens, W.E., Storey, M., Donaldson, C.H., Ellam, R.M., Lelikov, E., Tararin, G. & Garbe-Schoenberg, C., 2009. Age and origin of the Amirante ridge-trench structure, western Indian Ocean, in *Proceedings of the Fall Meeting 2009,* San Francisco, CA, USA, Am. Geophys. Un., Abstract T23A-1885.

Tararin, I.A. & Lelikov, E.P., 2000. Amirante island arc in the Indian Ocean: data on the initial island arc magmatism, *Petrology,* **8,** 53–65.

Todal, A. & Eldholm, O., 1998. Continental margin off Western India and Deccan large igneous province, *Mar. geophys. Res.,* **20,** 273–291.

Torsvik, T.H., Ashwal, L.D., Tucker, R.D. & Eide, E.A., 2001. Geochronology and palaeogeography of the Seychelles microcontinent: the India link, in *Assembly and Break-Up of Rodinia,* Vol. **100,** pp. 47–59, eds Meert, J.G. & Powell, C.M., Precambrian Res.

Torsvik, T.H., Müller, R.D., Van Der Voo, R., Steinberger, B. & Gaina, C., 2008. Global plate motion frames: toward a unified model, *Rev. Geophys.,* **46,** 1–44.

Torsvik, T.H. *et al.*, 2013. A Precambrian microcontinent in the Indian Ocean, *Nat. Geosci.,* **6**, 223–227.

Uenzelmann-Neben, G., Jokat, W., Miller, H. & Steinmetz, S., 1992. The Aegir Ridge: structure of an extinct spreading axis, *J. geophys. Res.,* **97,** 9203–9218.

van Hinsbergen, D.J.J., Steinberger, B., Doubrovine, P.V. & Gassmöller, R., 2011. Acceleration and deceleration of India-Asia convergence since the Cretaceous: roles of mantle plumes and continental collision, *J. geophys. Res.,* **116,** B06101, doi:10.1029/2010JB008051.

Wiens, D.A. *et al.*, 1985. A diffuse plate boundary model for Indian Ocean tectonics, *Geophys. Res. Lett.,* **12,** 429–432.

Yatheesh, V., Bhattacharya, G.C. & Mahender, K., 2006. The terrace like feature in the mid-continental slope region off Trivandrum and a plausible model for India–Madagascar juxtaposition in immediate pre-drift scenario, *Gondwana Res.,* **10,** 179–185.

Yatheesh, V., Bhattacharya, G.C. & Dyment, J., 2009. Early oceanic opening off Western India-Pakistan margin: the Gop Basin revisited, *Earth planet. Sci. Lett.,* **284,** 399–408.

Zatman, S., Gordon, R.G. & Richards, M.A., 2001. Analytic models for the dynamics of diffuse oceanic plate boundaries, *Geophys. J. Int.,* **145,** 145–156.